Inorganic Chemistry

ARTICLE

pubs.acs.org/IC

Refinement of the α-U_4O_9 Crystalline Structure: New Insight into the $U_4O_9 \rightarrow U_3O_8$ Transformation

L. Desgranges,*[,†] G. Baldinozzi,[‡,§] D. Siméone,[‡,§] and H. E. Fischer[⊥]

[†]CEA/DEN/DEC, Bat 352, Cadarache 13108, Saint Paul lez Durance, France

[‡]Matériaux Fonctionnels pour l'Energie, SPMS CNRS-Ecole Centrale Paris, 92295 Châtenay-Malabry, France

[§]CEA/DEN/DANS/DMN/SRMA/LA2M, 91191 Gif-sur-Yvette, France

[⊥]Institut Laue-Langevin, 6 rue Jules Horowitz, B.P. 156, 38042 Grenoble Cedex, France

Supporting Information

ABSTRACT:

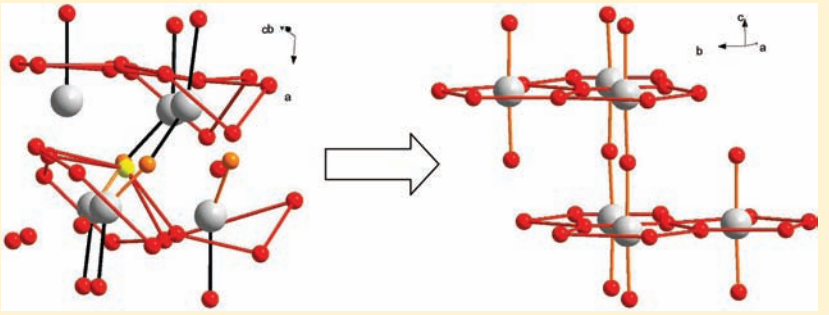

The oxidation reaction of UO_2 into U_3O_8 is studied as a function of the crystalline distortion of interstitial oxygen clusters, named cuboctahedra, which appear in U_4O_9 and U_3O_7 intermediate phases. For that purpose, the refinement of α-U_4O_9 was performed because this phase undergoes a trigonal distortion from cubic β-U_4O_9 when the temperature is decreased. In α-U_4O_9, the cuboctahedra can be described as crumpled sheets taken from a fragment of U_3O_8. The manner by which the accumulation of crumpled sheets can lead to the formation of U_3O_8 is discussed.

INTRODUCTION

The reaction of oxidation of UO_2 into U_3O_8 is of technological importance for the nuclear industry, both for reprocessing of fresh defective fuel and for dry storage of used nuclear fuel.[1] The kinetics of this reaction was characterized 40 years ago,[2] but the underlying atomic mechanisms are still under discussion. Allen and Holmes[3] first proposed that this reaction occurred as a shear transformation of the (111) dense planes of the face-centered-cubic (fcc) crystalline structure of UO_2. This interpretation was consistent with the crystallographic positions of the uranium atoms in both UO_2[4] and U_3O_8[5] structures. At that time, however, no information was available on the positions of the oxygen atoms in U_4O_9 and U_3O_7, the intermediate phases formed during the oxidation of UO_2 at temperatures of less than 400 °C.[2] Since then, following Bevan et al.'s pioneering work,[6] Cooper and Willis[7] determined the crystal structure of β-U_4O_9 (stable between 353 and 873 K), and Desgranges et al.[8] proposed a crystal structure for β-U_3O_7. These crystallographic refinements shed light on the existence of a complex cluster, named a cuboctahedron, that includes five oxygen interstitials,[9] with one being at the cluster's center (Figure 1). The stability of the cuboctahedron was discussed in comparison with single oxygen interstitials using first-principle methods[10−12] and molecular dynamics.[13] However, no clear relationship exists between fluorite-derived crystal structures (large supercells) and the crystal structure of U_3O_8 because the organization in the dense planes proposed by Allen and Holmes is not related to the distribution of cuboctahedra.

In fact, transformation from UO_2 into U_3O_8 results from the convolution of two different mechanisms: the accumulation of oxygen in the solid and the distortion of its crystalline lattice. In this paper, we will focus on the distortion of the crystalline lattice only. For that purpose, we decided to study the crystalline structure of α-U_4O_9 (space group $R3c$), which is a trigonal distortion of the cubic β-U_4O_9 (space group $F\bar{4}3d$). This trigonal distortion privileges the family of UO_2 dense planes perpendicular to the rhombohedral axis. Thus, information could be gained on how the crystalline lattice behaves during the transformation to U_3O_8.

Conradson et al.[14] performed X-ray absorption spectroscopy (XAS) experiments on several samples, having compositions ranging from UO_2 to U_4O_9, in order to study the uranium atom's local environment. Garrido et al.[15] performed neutron diffraction

Received: February 16, 2011
Published: June 02, 2011

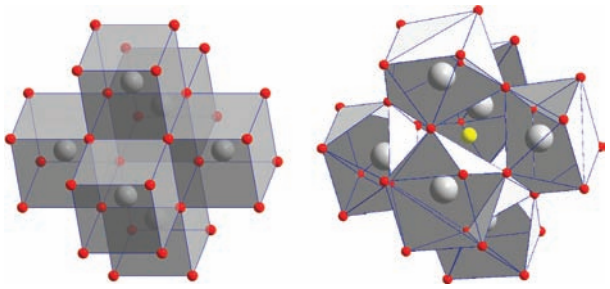

Figure 1. Comparison between the UO_2 lattice (left part) and a cuboctahedron in the β-U_4O_9 lattice (right part). Uranium atoms are gray, oxygen atoms are red, and the oxygen atom at the center of the cuboctahedron is yellow.

experiments at room temperature on a α-U_4O_9 sample, and they derived its pair distribution function (PDF). The PDF is a function of the interatomic distance r and relates the probability of finding an atom at a distance r from an average atom at the origin. However, the PDF averages over all atomic species and also over all crystallographic directions and thus provides some structural information, but no detailed crystal structure of α-U_4O_9 has been proposed so far.

Although α-U_4O_9 is a crystalline compound, it was not possible to use standard Rietveld analysis of neutron diffraction patterns that had been successful in the case of β-U_4O_9 because of the number of parameters to be refined is larger. In a low-symmetry structure, even though the crystallographic data included in the diffraction pattern are essentially the same in both phases, the PDF refinement is more robust than the Rietveld refinement. In the case of U_4O_9, PDF analysis is very interesting because the central oxygen atom has a very different local environment compared with those of other oxygen atoms. The central oxygen atom has a characteristic distance with other oxygen atoms at 3.3 Å, the distance of which does not overlap with those for oxygen atoms in the regular UO_2 lattice.

In this paper, we present the measurement and refinement of the PDF for U_4O_9 at room temperature. The results are discussed with respect to the transformation of UO_2 into U_3O_8.

EXPERIMENTAL SECTION

Sample Preparation. The U_4O_9 sample was prepared by heat treatment of a mixture of UO_2 and U_3O_8 powder. The relative mass fraction of UO_2 and U_3O_8 was chosen in order to get, on average, a $UO_{2.23}$ composition. The two powders were carefully mixed. They were loaded into a quartz tube. The quartz tube was vacuum-pumped and sealed. Then this powder underwent a heat treatment at 1050 °C. The obtained powder had a dark color. Its quality was checked by X-ray diffraction. The powder had a grain size of a few micrometers, as measured by optical microscopy.

Neutron Diffraction and PDF Determination. The neutron diffraction experiment was performed on the D4c neutron diffractometer[16] at the Institute Laue-Langevin (ILL), Grenoble, France. A mass of 14.04 g of U_4O_9 powder was put into a sample container consisting of an 8-mm-diameter vertical cylinder of 0.1-mm-thick vanadium foil with niobium stoppers at the top and bottom. This sample container was sufficiently sealed to prevent the powder from escaping but not sufficiently sealed to allow a vacuum to be pumped. The sample environment in the diffractometer was therefore ambient air. Several diffraction patterns were acquired in order to measure accurately the various sources of background scattering: first with no sample at all

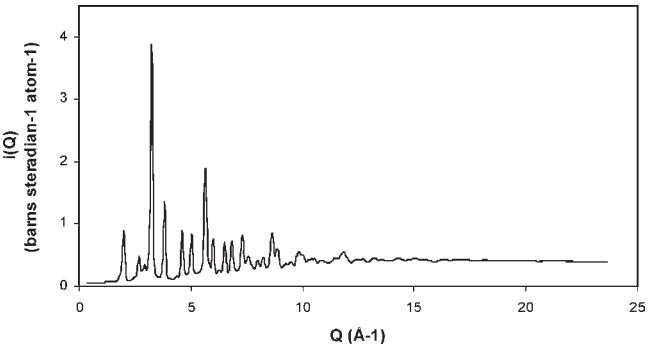

Figure 2. α-U_4O_9 neutron diffraction pattern corrected from air and sample holder diffusion.

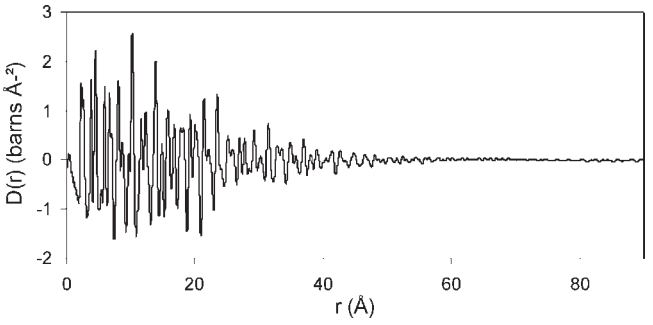

Figure 3. α-U_4O_9 $D(r)$ obtained by Fourier transformation (see the text for details).

(i.e., an empty diffractometer), then with an empty sample container, and last with the sample container filled with U_4O_9 powder, each for respective counting times of 4, 4, and 24 h. The stability of the diffraction pattern was checked by comparing data acquired at the same position and at different times. The neutron wavelength was determined by refinement of the diffraction pattern of a standard nickel sample and was found to be 0.4970 Å. The diffraction pattern was recorded up to Q_{max} = 23.5 $Å^{-1}$ (Figure 2).

The obtained diffraction pattern was treated to subtract the background due to air scattering and that due to scattering from the vanadium container, as well as the isotropic scattering coming from incoherent scattering that is subject to distortion from inelastic scattering effects (Placzek correction). A measurement of the sample height in the container gave the packing fraction, and by measurement of the diffraction from a vanadium standard, the diffraction pattern for the sample could be normalized onto an absolute scale of barns/sr/atom. The differential correlation function, $D(r)$, contains information relating to differences between the average density at a distance, r, from an average origin atom and the corresponding radial density for a homogeneous material. It was obtained for α-U_4O_9 (Figure 3) by Fourier transformation of this corrected diffraction pattern. The quality of this $D(r)$, as well as its amplitude normalization, was confirmed by comparing the slope of the PDF at r = 0 Å to the density of atoms per volume unit in the sample. The total distribution function $T(r)$ obtained from the α-U_4O_9 $D(r)$ is presented in Figure 4. A peak in $T(r)$ indicates an interatomic distance that occurs frequently in the sample, and its area is directly related to the coordination number for that distance.

Our $D(r)$ and $T(r)$ are very similar to those obtained by Garrido et al. measured at ISIS[15] although both experiments used very different experimental procedures. On the basis of these observations, our results were considered to be of sufficient quality for refinement of the α-U_4O_9 PDF.

dx.doi.org/10.1021/ic200316b |*Inorg. Chem.* 2011, 50, 6146–6151

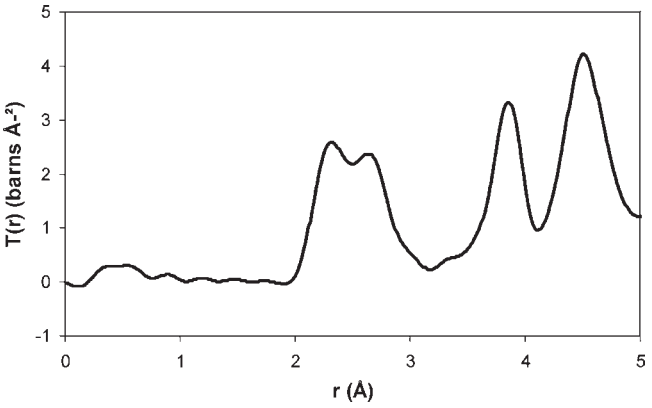

Figure 4. Zoom from 0 to 7 Å of the calculated α-U_4O_9 $T(r)$ (see the text for details).

Refinement Procedure. Our PDF for α-U_4O_9 was refined with *PDFGUI* software.[17] In such a minimization procedure, the crystalline structure used as the starting point has to be as close as possible to the actual crystalline structure.

According to Belbeoch et al.,[18] the room temperature phase of U_4O_9 is the result of a distortion of the cubic β phase that is very sensitive to the grain size. On the one hand, in fine-grain-size powder samples (<1 μm), the 4-fold superstructure lines, which are characteristic of the ordering of the cuboctahedra, reversibly disappear when the sample temperature is lowered below the $\alpha-\beta$ transition temperature with a significant trigonal distortion. On the other hand, in coarse-grained samples (≥1 μm), the lattice superstructure does not vanish and a smaller trigonal distortion is observed. Our sample belongs to this latter category; therefore, it seems reasonable to start with the high-temperature phase for determination of the room temperature structure. We have established the group−subgroup relationship between the cubic ($Ia\bar{3}d$) and most symmetric trigonal phase ($R3c$) space groups compatible with the diffraction pattern and used the lost symmetry elements to generate the atomic positions in the room temperature structure. In this structure, there are 75 independent atomic sites occupied by 22 uranium atoms and 48 oxygen atoms and 4 sites with $^1/_4$ occupancy for the oxygen atom at the center of the cuboctahedron. This crystalline structure was used to model the α-U_4O_9 neutron diffraction pattern, refining only the lattice parameters, which led to R_{Bragg} = 6.5%. That provided a good starting point from the point of view of Rietveld analysis. Unfortunately, no satisfactory refinement of the crystalline structure could be performed because of the large number of parameters.

In PDF analysis, two choices are possible for the position of the oxygen atom at the center of the cuboctahedron: either it shares disordered positions or it occupies only one of those possible sites. We chose to order this atom: therefore, the starting crystalline structure in the $R3c$ space group consists of 22 independent uranium atoms and 49 independent oxygen atoms.

In order to reduce the number of parameters to be refined, all uranium atoms were given a common isotropic thermal motion and all oxygen atoms were also given another common isotropic thermal motion. Nevertheless, the number of parameters associated with the atomic positions was still 207. The parameters describing instrumentation parameters were fixed to values appropriate for the D4 instrument: Q_{broad}, which describes the experimental peak broadening, was set to 0.03, and Q_{damp}, which describes the intensity dampening with increasing r, was set to 0.047. The high Q cutoff Q_{max} was set to 23.5 Å. Moreover, the ripples of the PDF for r < 1.6 Å were removed and replaced by a straight line, so that the PDF is essentially flat from 0 to 2 Å. With this procedure, we wanted to remove the unphysical ripples at low r that result from Fourier transformation of data having finite Q_{max}.

RESULTS

A first refinement was performed in which the positions of the 22 uranium and 49 oxygen atoms were refined with uranium and oxygen thermal motion. Refinement was performed up to χ^2 = 1.38 (χ^2 is a statistical indicator that should reach 1 for best refinements), but at that point, it led to too short distances to be physically relevant. One oxygen atom had a 1.4 Å distance with a uranium atom and a 1.7 Å distance with another oxygen atom. This can be explained as a result of displacement of the central oxygen atom of the cuboctahedron, which leaves the central position and repels another oxygen atom of the cuboctahedron. The latter oxygen atom has less space than that in β-U_4O_9 because the other atoms are already closely packed, and this leads to too short distances to the surrounding atoms.

Hence, this crystallographic model based on the $R3c$ space group does not, obviously, correspond well to the actual crystal structure of α-U_4O_9, but it reflects some of its main characteristics because the quality of the fit is rather good with χ^2 = 1.38. This can be interpreted in at least two different ways.

First, the $R3c$ space group might not be the actual space group of the crystal structure of our sample. Belbeoch et al. proposed the $R3c$ space group for the α-U_4O_9 sample whose unit cell parameters would lead to a splitting of the diffraction lines that we do not observe for our sample.[18] One reason for that could be the existence of correlations between the cuboctahedra that could be fully achieved or frustrated as a function of the sample history. Using the $R3c$ space group implies that displacement of the central oxygen atom is correlated for all cuboctahedra in the crystal. A space group with a lower symmetry or a larger supercell would be necessary to account for an uncorrelated central oxygen atom and could induce sufficient relaxation of the crystalline structure so that short atomic distances could be avoided.

Second, the oxygen content of our sample could be slightly different from the one expected from β-U_4O_9. U_4O_9 is known to be a nonstoichiometric compound whose oxygen/uranium ratio can vary from 2.23 to 2.25, with the exact ratio of β-U_4O_9 being 2.234375. This difference in the oxygen content could create different local concentrations, or frustration.

In order to obtain results that can be discussed independently of both the oxygen content and local symmetry, we chose to remove the oxygen atoms with unrealistic short bonds from the description of α-U_4O_9 in the $R3c$ space group. This does not provide the exact crystal structure of α-U_4O_9, but it gives at least an approximate description of frustration-free local areas.

Because of symmetry constraints, six oxygen atoms were removed. Thus, the initial chemical formula $U_{128}O_{286}$ of β-U_4O_9 became $U_{128}O_{280}$ corresponding to a ∼2% decrease in the oxygen content. A second refinement was then performed starting from the atomic positions previously refined in which these six oxygen atoms were removed. In this refinement, the previously refined thermal motion parameters were fixed: 0.0016 for u_U and 0.005 for u_O. Refinement was performed up to χ^2 = 1.21. The calculated PDF is compared to the measured one in the upper part of Figure 5. A detail plot between 0.5 and 7.5 Å is presented in the lower part of Figure 5.

The refined atomic positions of α-U_4O_9 are slightly displaced from the positions in β-U_4O_9, but the shift of the central atom associated with the suppression of six oxygen atoms leads to an arrangement of the oxygen atoms of the cuboctahedron that has a lot of similarities with the U_3O_8 crystal structure.

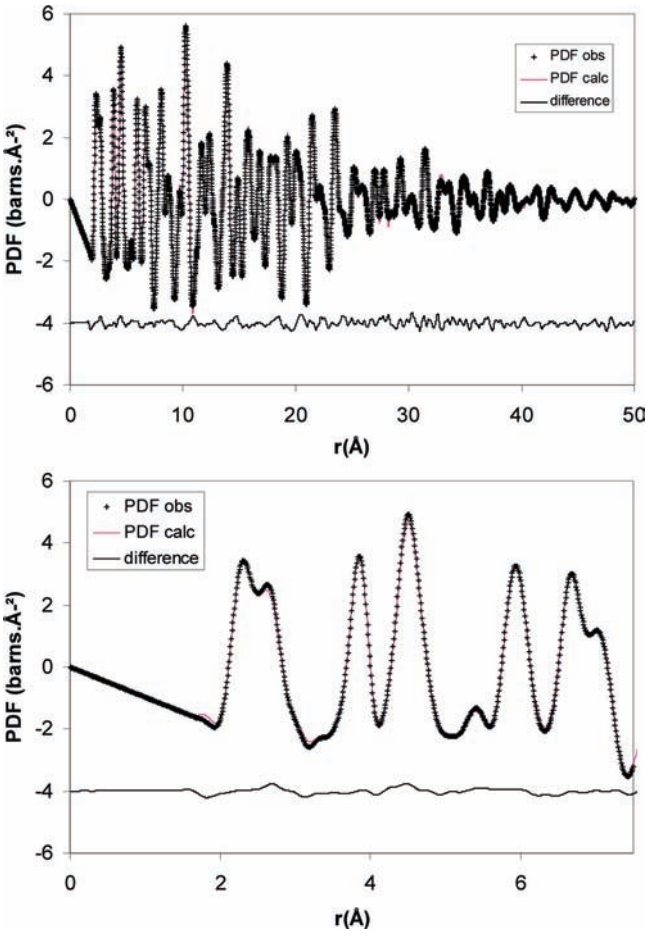

Figure 5. Comparison between the fitted PDF (purple line) and experimental PDF (crosses): top, the whole refined pattern; bottom, a zoom for r between 0 and 7.5 Å. The difference between the experimental and calculated points is given by a black line, which was shifted by −4 for better clarity.

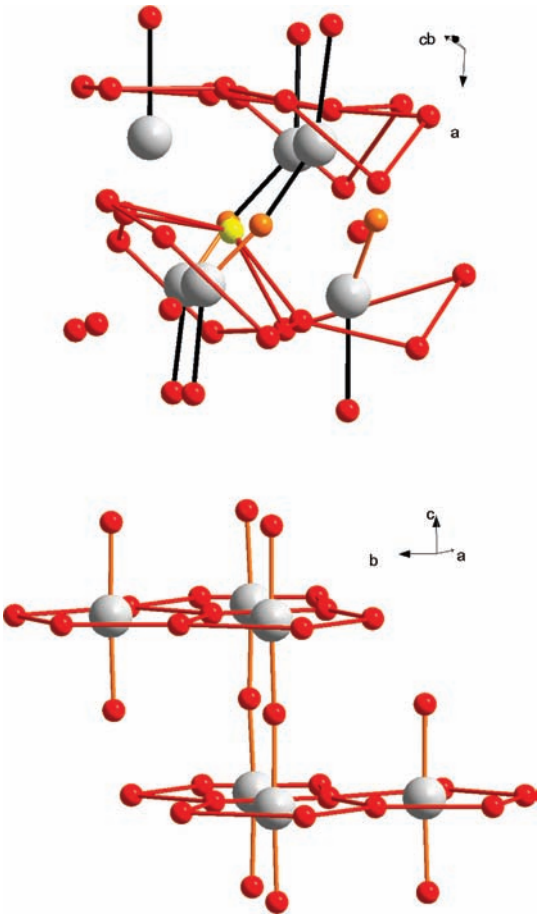

Figure 6. Comparison between the U_3O_8 encapsulated cluster in U_4O_9 (upper part) and the U_3O_8 fragment (lower part), which could be transformed by a shear strain. Uranium atoms are gray, and oxygen atoms are red, are orange for 1.8 Å short U−O bonds, and are yellow for the atom initially at the cuboctahedron center.

The displacement of the oxygen atom located in the center of the cuboctahedron in β-U_4O_9 induces a new organization of the atoms surrounding the cuboctahedron, which is depicted in Figure 6. In this figure, the six nearest uranium atoms are located on two dense planes, derived from UO_2 (111) planes, below and above the central oxygen atom, marked in yellow. Each uranium atom is surrounded by a distorted pentagon made of oxygen atoms more or less parallel to the dense planes. Each uranium atom is also connected to other oxygen atoms, forming U−O bonds perpendicular to the dense planes or linking uranium atoms from the two dense planes. Three U−O bonds, shown in orange, are formed at 1.8 Å; this bond length is usually observed for the U6+ cation in uranium oxo compounds.[19] This configuration of the six uranium atoms and their coordination polyhedra makes them resemble crumpled sheets taken from a fragment of U_3O_8. The corresponding fragment of U_3O_8 is represented in Figure 6. In U_3O_8, oxygen atoms form pentagons in the $a-b$ plane and UOU chains along the c axis.

DISCUSSION

The atomic positions obtained by refinement of the PDF give some new insight into the mechanism by which U_4O_9 is transformed into U_3O_8. The similarity between the U_4O_9 crumpled sheets and the U_3O_8 fragments shown in Figure 7 could indicate that transformation from U_4O_9 to U_3O_8 consists of stretching U_4O_9 crumpled sheets, which is consistent with the mechanism proposed by Allen and Holmes.[3] Because the sheets derived from U_3O_8 are crumpled in U_4O_9, they can be considered as mechanically strained by the surrounding atoms, which approximately keep the UO_2 crystallographic positions. Hence, the shear transformation from the fluorite-derived structure to the U_3O_8-layered structure should be viewed as a competition between frustrated crumpled sheets and the remaining UO_2 lattice shown in Figure 6. Two conditions are required for such a transformation to occur. First, the crumpled sheets must lie in the same plane, so that the shear transformation creates U_3O_8 in a sufficiently large domain. Second, the energetic balance must be in favor of U_3O_8, meaning that a minimum concentration of crumpled sheets should be reached. These conditions are discussed below for three different cases.

(1) α-U_4O_9 cannot undergo a shear transformation because the crumpled sheets are disoriented with respect to each other, at least in our data. Nevertheless, Belbeoch et al.[18] observed α-U_4O_9 with a large rhombohedral distortion with a grain size of under 1 μm (the exact value is not known). This size effect could be understood by considering that, below a minimal size, the orientation of the crumpled sheets is not imposed by the bulk

dx.doi.org/10.1021/ic200316b |*Inorg. Chem.* 2011, 50, 6146–6151

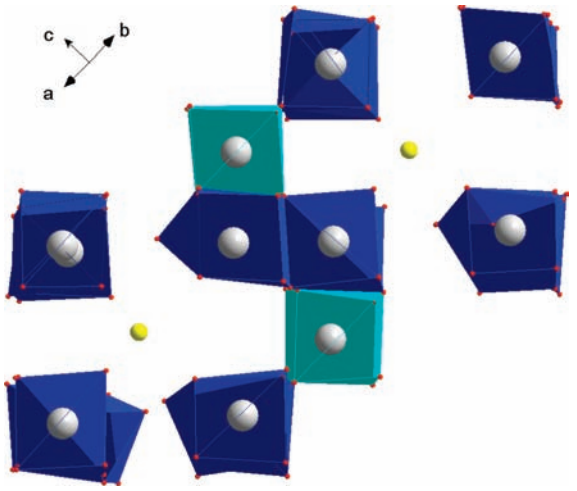

Figure 7. Coordination polyhedra of the remaining uranium atoms around the crumpled sheets. Uranium atoms are gray, and the oxygen atoms that they are linked to are represented as small red dots. The oxygen atom initially at the center of the cuboctahedron is yellow. The coordination polyhedron of uranium atoms are dark blue when they share one face with the cuboctahedron and light blue when they share no face with it.

symmetry but by surface effects. Thus, they could be aligned, leading to a cooperative effect that would stretch the crumpled sheets. This size effect could also explain the different PDFs measured on α-U_4O_9. In our samples, the grain size is more than 1 μm. Garrido prepared his sample by a high-temperature route in a manner similar to what we did. Consistently, his results, cubic α-U_4O_9, and his PDF are very similar to ours and can be associated with grain sizes bigger than 1 μm. Conradson prepared his XAS samples by a high-temperature route, followed by a grinding phase. The grain size of the obtained powder is not given in the paper, but if it was less than 1 μm, in the PDF he obtained a significant number of short U−O bonds that could be related to the heavily distorted lattice, as first shown by Belbeoch et al. The importance of the route used for preparing the samples was also evidenced by Raman spectroscopy data. Manara and Renker[20] and He and Shoesmith[21] both prepared samples of overstoichiometric UO_2 by heat treating UO_2 specimens in an oxidizing atmosphere at high temperature. He and Shoesmith found a 630 cm^{-1} band in their Raman spectrum, while Manara and Renker did not.

(2) The formation of U_3O_8 involves different crystalline phases as a function of the temperature. At high temperature, U_3O_8 forms directly on UO_2. This can be understood by considering that thermal motion makes UO_2 dense layers loose and that a cuboctahedron induces shear transformation of UO_2 as soon as it is created. At a temperature lower than 400 °C, U_3O_8 appears only after a layer of U_3O_7 is formed. The U_3O_7 crystal structure is a UO_2-derived structure with 16 cuboctahedra per unit cell instead of 12 cuboctahedra per unit cell as in β-U_4O_9. U_3O_7 is a metastable compound stabilized by the mechanical stresses induced by its formation on the UO_2 surface.[22] This can be understood by considering the energy balance inside the U_3O_7 layer: more energy is needed to achieve a shear transformation that is hindered by the tensile stress in the layer. This shear transformation can only occur when this tensile stress is relaxed by cracking the U_3O_7 layer.[22]

(3) Doping UO_2 with trivalent cations is known to limit U_3O_8 formation. Assuming that doping leads to a random distribution of trivalent cations, it will hinder the formation of cuboctahedra because it requires six surrounding uranium atoms with 5+ oxidation number. Thus, cuboctahedra cannot be formed at any position, and their cooperative effect for shear transformation is thereby reduced.

CONCLUSION

The neutron PDF for α-U_4O_9 was obtained by Fourier transformation of the neutron diffraction data obtained on the D4 instrument at the ILL. This PDF was refined, and we have proposed a description of the crystal structure of α-U_4O_9 in an area free from mechanical stress and chemical frustration. This description provides new insight into the interpretation of the transformation of U_4O_9 to U_3O_8, which would be driven by the shear transformation of crumpled sheets, associated with cuboctahedra, into regular U_3O_8 sheets.

ASSOCIATED CONTENT

Supporting Information. X-ray crystallographic data in CIF format. This material is available free of charge via the Internet at http://pubs.acs.org.

AUTHOR INFORMATION

Corresponding Author
*E-mail: Lionel.desgranges@cea.fr.

ACKNOWLEDGMENT

The authors are indebted to the program MATAV funded by CEA, which supported this study. We also thank the technical staff and radioprotection personnel of the ILL for their contributions to the neutron diffraction work.

REFERENCES

(1) Ferry, C.; Poinssot, C.; Cappelaere, C.; Desgranges, L.; Jegou, C.; Miserque, F.; Piron, J. P.; Roudil, D.; Gras, J. M. *J. Nucl. Mater.* **2006**, *352*, 246.
(2) McEachern, R. J.; Taylor, P. *J. Nucl. Mater.* **1998**, *254*, 87.
(3) Allen, G. C.; Holmes, N. R. *J. Nucl. Mater.* **1995**, *223*, 231.
(4) Willis, B. T. M. *J. Phys.* **1964**, *25*, 431.
(5) Loopstra, B. O. *Acta Crystallogr.* **1964**, *17*, 651.
(6) Bevan, D. J. M.; Grey, I. E.; Willis, B. T. M. *J. Solid State Chem.* **1986**, *61*, 1.
(7) Cooper, R. I.; Willis, B. T. M. *Acta Crystallogr.* **2004**, *A60*, 322–325.
(8) Desgranges, L.; Baldinozzi, G.; Rousseau, G.; Niepce, J.-C.; Calvarin, G. *Inorg. Chem.* **2009**, *48*, 7585–7592.
(9) Murray, A. D.; Willis, B. T. M. *J. Solid State Chem.* **1990**, *84*, 52–57.
(10) Geng, H. Y.; Che, Y.; Kaneta, Y.; Kinoshita, M. *Phys. Rev. B* **2008**, *77*, 180101.
(11) Geng, H. Y.; Che, Y.; Kaneta, Y.; Kinoshita, M. *Appl. Phys. Lett.* **2008**, *93*, 201903.
(12) Andersson, D. A.; Lezema, J.; Uberuaga, B. P.; Deo, C.; Conradson, S. D. *Phys. Rev. B* **2009**, *79*, 024110.
(13) Yakub, E.; Ronchi, C.; Staicu, D. *J. Nucl. Mater.* **2009**, *389*, 119–126.
(14) Conradson, S. D.; et al. *Inorg. Chem.* **2004**, *43*, 6922–6935.
(15) Garrido, F.; et al. *Inorg. Chem.* **2006**, *45*, 8408–8413.
(16) Fischer, H. E.; Cuello, G. J.; Palleau, P.; Feltin, D.; Barnes, A. C.; Badyal, Y. S.; Simonson, J. M. *Appl. Phys. A: Mater. Sci. Process.* **2002**, *74*, S160–S162.

(17) Farrow, C. L.; et al. *J. Phys.: Condens. Matter* **2007**, *19*, 335219.
(18) Belbeoch, B.; Boivineau, J. C.; Perio, P. *J. Phys. Chem. Solids* **1967**, *28*, 1267–1275.
(19) Burns, P. C. . In *Structural chemistry of inorganic actinide compounds*; Krivovichev, S. V., Burns, P. C., Tananaev, I. G., Eds.; Elsevier: New York, 2007.
(20) Manara, D.; Renker, B. *J. Nucl. Mater.* **2003**, *321*, 233–237.
(21) He, H.; Shoesmith, D. *Phys. Chem. Chem. Phys.* **2010**, *12*, 8108–8117.
(22) Desgranges, L.; Palancher, H.; Gamaléri, M.; Micha, J. S.; Optasanu, V.; Raceanu, L.; Montesin, T.; Creton, N. *J. Nucl. Mater.* **2010**, *407*, 44–47.